Limnological Analysis of Big Round Lake WI during Alum Application: 2024 interim report

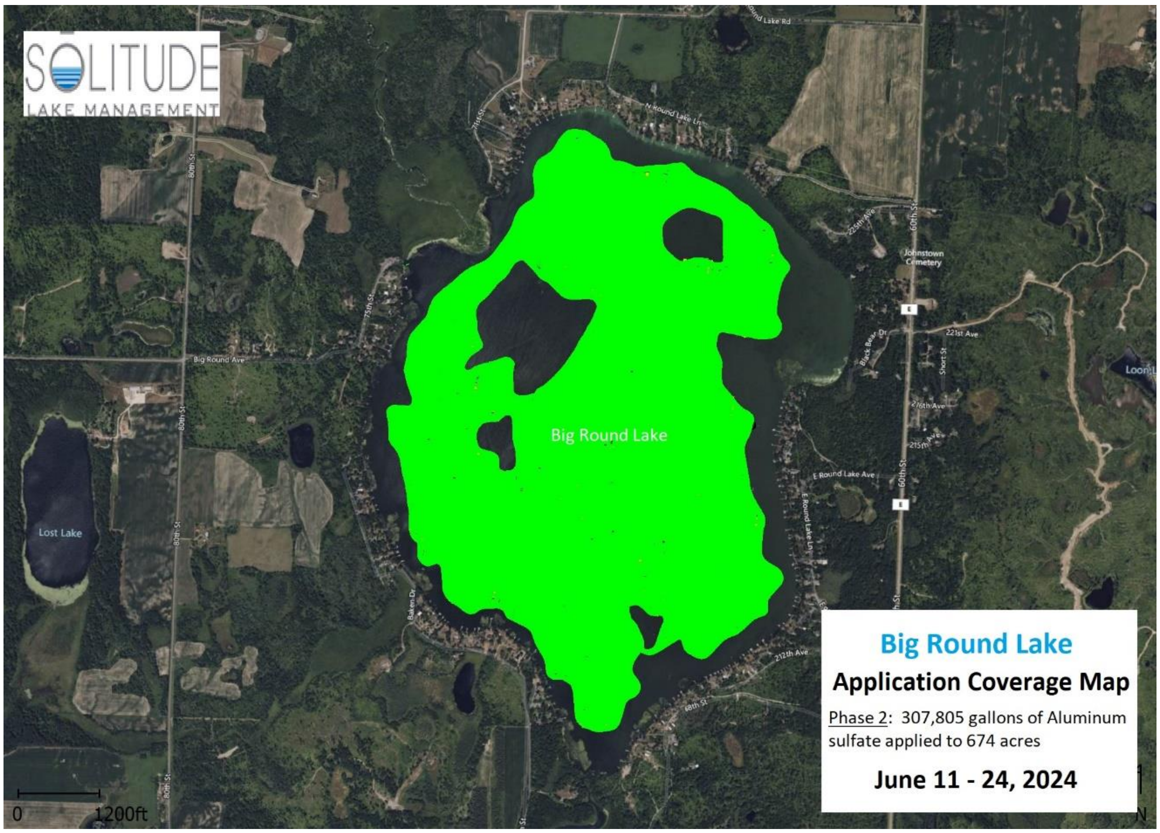

The 2024 alum application coverage map. Credit: Solitude Lake Management

5 December 2024

University of Wisconsin - Stout
Center for Limnological Research and Rehabilitation
Menomonie, Wisconsin 54751
715-338-4395
jamesw@uwstout.edu

1.0 EXECUTIVE SUMMARY.

- Big Round Lake was treated with 307,805 gallons of aluminum sulfate over 674 ac (i.e., > 10-ft depth contour) between 11 and 24 June 2024. The application represented the second of four 25 g/m^2 Al doses to the lake.
- The 2024 alum application coincided with undetectable bottom SRP concentrations between June and September, indicating low internal P loading from sediments stored in the lake.
- Chlorophyll concentrations were very low throughout the summer period, ranging between 1.5 µg/L and 22 µg/L between July and September. The mean over this period was only 7.8 µg/L and chlorophyll bloom exceedance frequency was only 8% for a concentration > 20 µg/L.

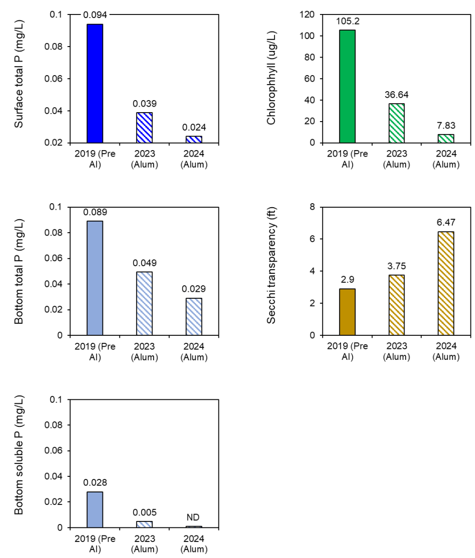

Mean summer (July-September) water quality variables before (2019) and during (2023-24) the first and second alum application.

- Overall, Big Round Lake exhibited substantial improvement in water quality during the second alum application compared to summer (JUL-SEP) limnological conditions in 2019 (i.e., before treatment). Mean summer surface total P declined by 74% to 0.024 mg/L (from 0.094 mg/L in 2019). Mean summer bottom total P and soluble P declined by 67% and nearly 100%, respectively in 2024. Mean summer chlorophyll declined to 7.8 µg/L in 2024 compared to 105 µg/L in 2019, representing a 93% improvement. Secchi transparency increased from a summer mean of 2.9 ft in 2019 to 6.47 ft in 2024 (123% improvement).
- The 2024 alum treatment also coincided with reduced summer bloom frequency exceedance. Compared to the pretreatment year 2019, blooms exceeding 30 µg/L fell from 83% to only 3%, blooms exceeding 40 µg/L declined from 74% to 1, and blooms exceeding 50 µg/L decreased from 67% to <1%. Thus, the second year of alum application led to substantial reduction in severe cyanobacteria blooms.

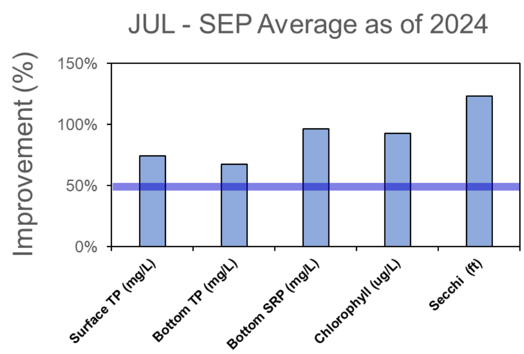

Percent improvement in various limnological variable in 2024 versus 2019 pretreatment means. Horizontal blue bar denotes 50% improvement for comparison.

- Evidence of a surface Al floc layer was observed at all stations after the alum application. Concentrations aluminum-bound P, which represented P bound to the Al floc layer, were generally highest in the upper 4-cm sediment layer. Aluminum-bound P concentrations were much more uniform spatially in the lake in 2024 compared to 2023, ranging between 0.42 and 0.77 g/m^2.
- Generally, laboratory-derived P flux from anaerobic sediment declined after the 2nd alum application in 2024, compared to fluxes measured in 2023 after the 1st alum treatment. The mean over all sediment stations was low at 1.4 mg/m^2 d (± 0.25 standard error, SE) in 2024, compared 2.48 mg/m^2 d (± 0.50 SE) in 2023 and 2.48 mg/m^2 d (± 0.58 SE) in 2019-2020. The 2024 decline in anaerobic P flux from sediment represented a 43% improvement over the mean pretreatment P flux. Additional alum applications should result in uniformly lower P flux over time.

2.0 OBJECTIVES.

The objectives of these investigations were to examine lake and sediment response to the second of four partial alum applications to Big Round Lake. A 100 g/m^2 alum dosage to depths greater than the 10-ft contour (674 ac) was prescribed to control internal P loading. The Al dose was split into four successive 25 g/m^2 treatments to be applied annually between 2023-2026. Dose splitting and annual applications should maximize the binding of sediment P onto the Al floc layer in the surface sediments (Lewandoski et al. 2003, de Vicente et al. 2008a, Huser 2012, Jensen et al. 2015, James and Bischoff 2015, James 2017a) and reduce availability and direct uptake of mobile sediment P to cyanobacteria for growth. The first partial alum application occurred to Big Round Lake between 13 – 27 June 2023. The second partial alum dose was applied between 11 – 24 June 2024 (*Cover figure*).

3.0 METHODS.

In-lake monitoring

Water samples for limnological variables were collected at a centrally-located station in the deepest portion of the lake (Fig. 1). Samples were collected biweekly between June and the end of September. An integrated sample was collected over the upper 2-m for analysis of total phosphorus and chlorophyll a. An additional discrete sample was collected within 0.5 m of the sediment surface for analysis of total and soluble reactive P. Secchi transparency and in situ measurements (temperature, dissolved oxygen, pH, and conductivity at 0.5-m intervals) were also collected on each date.

Samples for total P were digested with potassium persulfate prior to analysis (APHA 2011). Samples for soluble reactive P were filtered immediately in the field using a 0.45 µm pore size syringe filter. Phosphorus was analyzed on a Perkin-Elmer UV-VIS Lambda 25 Spectrophotometer using the ascorbic acid method (APHA 2011). Samples for chlorophyll analysis were filtered onto a type A/E glass fiber filter, extracted in 90% acetone overnight in the freezer, and analyzed fluorometrically using a TD 300 fluorometer (Turner Designs).

Laboratory-derived rates of P release from sediment

Sediment cores were collected at the WQ sampling station and 7 additional stations in Big Round Lake (Fig. 1) for determination of diffusive P flux from sediment under controlled laboratory conditions (James 2017b). Cores were carefully drained of overlying water in the laboratory and the upper 10 cm of sediment were transferred intact to a smaller acrylic core liner (6.5-cm dia and 20-cm ht) using a core remover tool. Surface water collected from each lake was filtered through a glass fiber filter (Gelman A-E), with 300 mL then siphoned onto the sediment contained in the small acrylic core liner without causing sediment resuspension. They were placed in a darkened environmental chamber and incubated at a constant temperature of ~20 ^{o}C to reflect summer conditions. The Eh environment in the overlying water was controlled by gently bubbling nitrogen-CO_2 (anaerobic) through an air stone placed just above the sediment surface in each system. Bubbling action insured complete mixing of the water column but not disrupt the sediment.

Water samples for soluble reactive P were collected from the center of each system using an acid-washed syringe and filtered through a 0.45 µm membrane syringe filter. The water volume removed from each system during sampling was replaced by addition of filtered lake water preadjusted to the proper oxidation-reduction condition. These volumes were accurately measured for determination of dilution effects. Soluble reactive P was measured colorimetrically using the ascorbic acid method (APHA 2011). Rates of P release from the sediment (mg/m^2 d) were calculated as the linear change in mass in the overlying water divided by time (days) and the area (m^2) of the incubation core liner. Regression analysis was used to estimate rates over the linear portion of the data.

Evaluation of sediment P characteristics

The objectives of this task were to quantify vertical variations in sediment textural characteristics and mobile P fractions involved in sediment internal P loading to the overlying water column. Sediment cores were sectioned at 2-cm intervals over the upper 10 cm for analysis of sediment physical-textural characteristics and P fractions. Sediment sections were analyzed for moisture content, sediment density, organic matter content, loosely-bound P, iron-bound P, labile organic P, and aluminum-bound P. Subsamples were dried at 105 °C to a constant weight and burned at 550 °C for determination of moisture content, sediment density, and organic matter content (Håkanson and Jensson 2002). Phosphorus fractionation was conducted according to Psenner and Puckso (1988) and Hjieltjes and Lijklema (1980) for the determination of ammonium-chloride-extractable P (1 M NH_4Cl; loosely-bound P), bicarbonate-dithionite-extractable P (0.11 M BD; iron-bound P), and sodium hydroxide-extractable P (0.1 N NaOH; aluminum-bound and labile organic P). Sediment total aluminum was analyzed via inductively-coupled plasma atomic absorption spectropohometry using EPA method 6010D after digestion according to EPA method 3050B.

The loosely-bound and iron-bound P fractions are readily mobilized at the sediment-water interface under anaerobic conditions that result in desorption of P from bacterially-reduced iron compounds (i.e., Fe^{+3} to Fe^{+2}) in the sediment and diffusion into the overlying water column (Mortimer 1971, Boström 1984, Nürnberg 1988). The sum of these fractions are referred to as redox-sensitive P (i.e., redox-P; the P fraction that is active in P release under anaerobic and reducing conditions). In addition, labile organic P

(LOP) can be converted to soluble P via bacterial mineralization or hydrolysis of bacterial polyphosphates to soluble phosphate under anaerobic conditions (Gächter et al. 1988; Gächter and Meyer 1993; Hupfer et al. 1995). The sum of redox-P and LOP is collectively referred to a biologically-labile P. This fraction is generally active in recycling pathways that result in exchanges of phosphate from the sediment to the overlying water column and potential assimilation by algae.

4.0 RESULTS.

Lake limnological response

Local precipitation (measured at Amery, Cumberland, and Luck WI) more than 1 inch occurred in late March, mid- and late April, mid- and late May, mid-June, early July, and early and late August 2024 (Fig. 2). A period of drought occurred in mid-July. Daily precipitation exceeded 2 inches during storms in mid-May, early June, and early and late August. Monthly precipitation at Amery in 2024 was above the long-term average in May, June, and August, and well below the average in July and September (Fig. 3).

Big Round Lake stratification occurred in late June and extended into late July (Fig. 4). Bottom anoxia developed in conjunction with this stratification period and extended to the ~ 3.5-m depth by mid-July. Alum application was initiated on 11 June, before strong stratification developed. A period of complete water column mixing occurred in late-July to early August, resulting in reoxygenation of the entire water column. Periods of weak stratification in August resulted in bottom anoxia. Fall turnover occurred in September.

Despite periods of summer bottom anoxia, total and soluble P concentrations remained low in the bottom waters in conjunction with the second alum application (Fig. 5). Bottom total P concentrations ranged between 0.018 mg/L and 0.040 mg/L and bottom soluble P concentrations were below detection limits throughout the summer of 2024,, indicating limited internal P loading for cyanobacterial uptake.. By comparison, Big

Round Lake exhibited relatively high bottom SRP concentration between late July and early August 2019 (i.e., before the first alum application, Fig. 5).

Surface concentrations of total P were much lower in 2024 compared to the pretreatment summer of 2019 (Fig. 6). Concentrations were below the WisCALM (2024) target of a mean 0.04 mg/L. Concentrations ranged between 0.018 mg/L and 0.030 mg/L between July and September. Low surface total P coincided with very low chlorophyll concentrations throughout the summer (Fig. 7). Chlorophyll ranged between 1.5 μg/L and 22 μg/L. As a result of low chlorophyll, Secchi transparency was much improved in 2024, ranging between 4.9 ft and 10.2 ft (1.5 m and 3.1 m, Fig. 8).

Regression relationships between surface chlorophyll and total P indicated that the second alum application had a very positive impact on P limitation of algal growth (Fig. 9). Much more severe P limitation of algal growth occurred during the summer of 2024 compared to 2019. Lower P-limited chlorophyll concentrations in 2024 also translated into great Secchi transparency compared to the pretreatment year 2019 (Fig. 9).

Mean summer (JUL-SEP) limnological response variables improved substantially in 2024 versus 2019 in conjunction with the second alum treatment (Fig. 10 and Table 1). Compared to 2019, mean surface total P and chlorophyll declined by nearly 60% and 65%, respectively (Fig. 11), to 0.039 mg/L and 36.6 μg/L in 2023. Mean summer bottom total P and soluble P declined to 0.03 mg/L and not detectable, respectively in response to the 2024 alum treatment, representing a 67% and 96% improvement (Fig. 11). Mean chlorophyl was only 7.8 μg/L, a 93%

Table 1. Summary of changes to Big Round Lake water quality after the first and second alum treatments in 2023 and 2024.

Variable	2019 (Pre Al)	2023 (Alum)	2024 (Alum)	Percent improvement (Pre Al versus 2024)
Surface TP (mg/L)	0.094	0.039	0.024	74%
Bottom TP (mg/L)	0.089	0.049	0.029	67%
Bottom SRP (mg/L)	0.028	0.005	0.001	96%
Chlorophyll (ug/L)	105.2	36.64	7.83	93%
Secchi (ft)	2.9	3.75	6.47	123%

improvement over the 2019 mean. Secchi transparency improved by 123% in 2024 versus 2019 to 6.47 ft.

A comparison of monthly means (pretreatment 2019 versus 2024) indicated that the severity of water quality impairment in Big Round Lake was reduced substantially during the 2024 alum treatment, particularly in August and September (Fig. 12). In addition, the percent of the summertime that chlorophyll blooms exceeded 30 μg/L, 40 μg/L, and 50 μg/L were considerably reduced in conjunction with the 2024 alum application to only 3%, 1%, and < 1%, respectively (Fig. 13).

Seasonal increases in summer lakewide P mass declined substantially in 2024 in conjunction with the second alum treatment (Fig. 14). Indeed, lake P mass actually declined between July and September. In contrast, the pretreatment lakewide summer P mass increase was 14.5 kg/d in 2019.

Sediment characteristics and diffusive phosphorus flux

Vertical patterns in sediment moisture content for sediment cores collected at the water quality station suggested the alum floc layer was located at the sediment surface (Fig. 15). Since the Al floc layer is only slightly denser than water at 1.01 to 1.02 g/cm^3, relatively high shear stress and turbulence would be required to induce mixing and incorporation into the original much denser sediment surface layer (James 2017). Moisture content of the sediment, a surrogate of density, was highest in the upper 4-cm sediment layer of sediment collected after the 2024 alum treatment, suggesting the Al floc layer was residing on top of the original sediment interface (Fig. 15). Aluminum-bound P concentrations (a surrogate measure of the alum floc layer) were highest at the sediment surface at 0.37 mg/g (Fig. 15).

Other stations exhibited peaks in aluminum and aluminum-bound P (Fig. 17 and 18), primarily within the surface sediment layer. In 2023, after the 1st Al application, concentrations peaks occurred primarily in the upper 2-cm sediment layer. After the 2nd

Al application in 2024, the concentration maximum expanded to the upper 4-cm surface sediment layer. However, concentrations were variable spatially with stations 10, 20, 50, 60, 70, and WQ exhibiting the highest surface concentration peaks, while stations 30 and 40 surface concentration peaks were lower (Table 2). Even though alum was precisely and evenly applied over the entire area, post-application movement is possible and had been well documented in other lakes treatment with alum (Egemose et al. 2009, Egemose et al. 2013, Huser 2017). Post application movement of the very low density newly-formed Al floc can occur via wind and wave activity and other turbulent processes. Additional application in 2025 and 2026 should result in more even distribution over the target area.

Table 2. Variations in aluminum and aluminum-bound P concentrations in the surface sediment layer at various stations in Big Round Lake in 2024.

Station	Al floc layer (cm)	Al (g/m^2)	Al-bound P (g/m^2)	Al:P ratio
WQ	4	20.0	0.454	44
10	4	19.6	0.339	58
20	4	16.2	0.329	49
30	2	10.5	0.196	54
40	4	17.8	0.341	52
50	4	18.8	0.315	60
60	4	18.0	0.316	57
70	4	21.7	0.358	61

Laboratory-derived anaerobic diffusive P fluxes declined at most stations in 2024 compared to rates measured in 2023 (Fig. 19). However, anaerobic P fluxes were higher in 2024 versus 2023 at station 20 and 30. In addition, anaerobic P fluxes were somewhat higher at the WQ station and 10 compared to pretreatment fluxes measured in 2019-2020 (Fig. 19). At other stations, anaerobic diffusive P flux in 2024 declined relative to fluxes measured in 2019. Overall, lakewide mean anaerobic diffusive P flux declined by 40% in 2024 in conjunction with the second alum application, compared to the 2019 mean (Fig. 20).

4.0 CONCLUSIONS AND RECOMMENDATIONS

The 2024 Al application to Big Round Lake represented the second of four 25 g/m^2 treatments that have or will be applied annually between 2023 and 2026. Compared to the pretreatment year, 2019, mean summer (i.e., JUL-SEP) limnological response variables were much improved in 2024 in conjunction with the second 25 g/m^2 alum application. The second alum application in 2024 entirely suppressed hypolimnetic P accumulation throughout the summer despite bottom anoxia. Relative to 2019, mean summer surface total P declined by 74% to 0.024 mg/L (from 0.094 mg/L in 2019). Mean summer bottom total P and soluble P declined by 67% and nearly 100%, respectively in 2024. Mean summer chlorophyll declined to only 7.8 μg/L in 2024 compared to 105 μg/L in 2019, representing a 93% improvement. Secchi transparency increased from a summer mean of 2.9 ft in 2019 to 6.5 ft in 2024 (123% improvement).

The overall alum application strategy was to split the estimated 100 g/m^2 Al dose into four 25 g/m^2 applications to 1) improved P binding efficiency and capacity onto the Al floc by subjecting consecutive annual low dose applications to sediment P, thereby, saturating binding sites on the Al floc with P and 2) suppress cyanobacteria blooms during the application process. Many cyanobacteria form resting stages as akinetes or spores that reside in the sediment and germinate under optimal environmental conditions. These resting stages may directly assimilate sediment P in excess of growth requirements and develop extensive blooms when germinated and mixed into the water column (Istvanovics et al. 1993, 2000; Pettersson et al. 1993; Perakis et al. 1996; Cottingham et al. 2015). Thus, controlling sediment P with consecutive annual alum treatments represents an application strategy designed to limit cyanobacteria access to sediment P in Big Round Lake. The 3nd consecutive alum application at 25 g/m^2 over 674 ac is scheduled for June 2025.

5.0 REFERENCES.

APHA (American Public Health Association). 2011. Standard Methods for the Examination of Water and Wastewater. 22th ed. American Public Health Association, American Water Works Association, Water Environment Federation.

Boström B. 1984. Potential mobility of phosphorus in different types of lake sediments. Int Revue Ges Hydrobiol 69:457-474.

de Vicente I, Huang P, Andersen FØ, Jensen HS. 2008a. Phosphate adsorption by fresh and aged aluminum hydroxide. Consequences for lake restoration. Environ Sci Technol 42:6650-6655.

de Vicente I, Jensen HS, Andersen FØ. 2008b. Factors affecting phosphate adsorption to aluminum in lake water: Implications for lake restoration. Sci Total Environ 389:29-36.

Egemose SG, Wauer G, Kleeberg A. 2009. Resuspension behavior of aluminum treated lake sediments: effects of aging and pH. Hydrobiologia 636: 203-217.

Egemose SG, Reitzel K, Andersen FØ, Jensen HS. 2013. Resuspension-mediated aluminum and phosphorus distribution in lake sediments after aluminum treatment. Hydrobiologia 701: 79-88.

Huser BJ. 2012. Variability in phosphorus binding by aluminum in alum treated lakes explained by lake morphology and aluminum dose. Wat Res 46:4697-4704.

Huser BJ. 2017. Aluminum application to restore water quality in eutrophic lakes: maximizing binding efficiency between aluminum and phosphorus. Lake Reserv Manage 33: 143-151.

Gächter R., Meyer JS, Mares A. 1988. Contribution of bacteria to release and fixation of phosphorus in lake sediments. Limnol Oceanogr 33:1542-1558.

Gächter R, Meyer JS. 1993. The role of microorganisms in mobilization and fixation of phosphorus in sediments. Hydrobiologia 253:103-121.

Håkanson L, Jansson M. 2002. Principles of lake sedimentology. The Blackburn Press, Caldwell, NJ USA

Hjieltjes AH, Lijklema L. 1980. Fractionation of inorganic phosphorus in calcareous sediments. J Environ Qua. 8: 130-132.

Hupfer M, Gächter R., Giovanoli R. 1995. Transformation of phosphorus species in settling seston and during early sediment diagenesis. Aquat Sci 57:305-324.

James WF. 2017a. Phosphorus binding dynamics in the aluminum floc layer of Half Moon Lake, Wisconsin. Lake Reserv Manage 33:130-142.

James WF. 2017b. Diffusive phosphorus fluxes in relation to the sediment phosphorus profile in Big Traverse Bay, Lake of the Woods. Lake Reserv Manage 33:360-368.

James WF, Bischoff JM. 2015. Relationships between redox-sensitive phosphorus concentration in sediment and the aluminum:phosphorus binding ratio. Lake Reserv Manage 31:339-346.

Jensen HS, Reitzel K, Egemose S. 2015. Evaluation of aluminum treatment efficiency on water quality and internal phosphorus cycling in six Danish lakes. Hydrobiologia 751:189-199.

Lewandowski J, Schauser I, Hupfer M. 2003. Long term effects of phosphorus precipitations with alum in hypereutrophic Lake Süsser See (Germany). Wat Res 37:3194-3204.

Mortimer CH. 1971. Chemical exchanges between sediments and water in the Great Lakes – Speculations on probable regulatory mechanisms. Limnol. Oceanogr 16:387-404.

Nürnberg GK. 1988. Prediction of phosphorus release rates from total and reductant-soluble phosphorus in anoxic lake sediments. Can J Fish Aquat Sci 45:453-462.

Psenner R, Puckso R. 1988. Phosphorus fractionation: Advantages and limits of the method for the study of sediment P origins and interactions. Arch Hydrobiol Biel Erg Limnol 30:43-59.

Rydin E, Huser B, Welch EB. 2000. Amount of phosphorus inactivated by alum treatments in Washington Lakes. Limnol Oceanogr 45:226-230.

WisCALM. 2019. Wisconsin 2020 consolidated assessment and listing methodology (WisCALM). Wisconsin Department of Natural Resources April 2019.

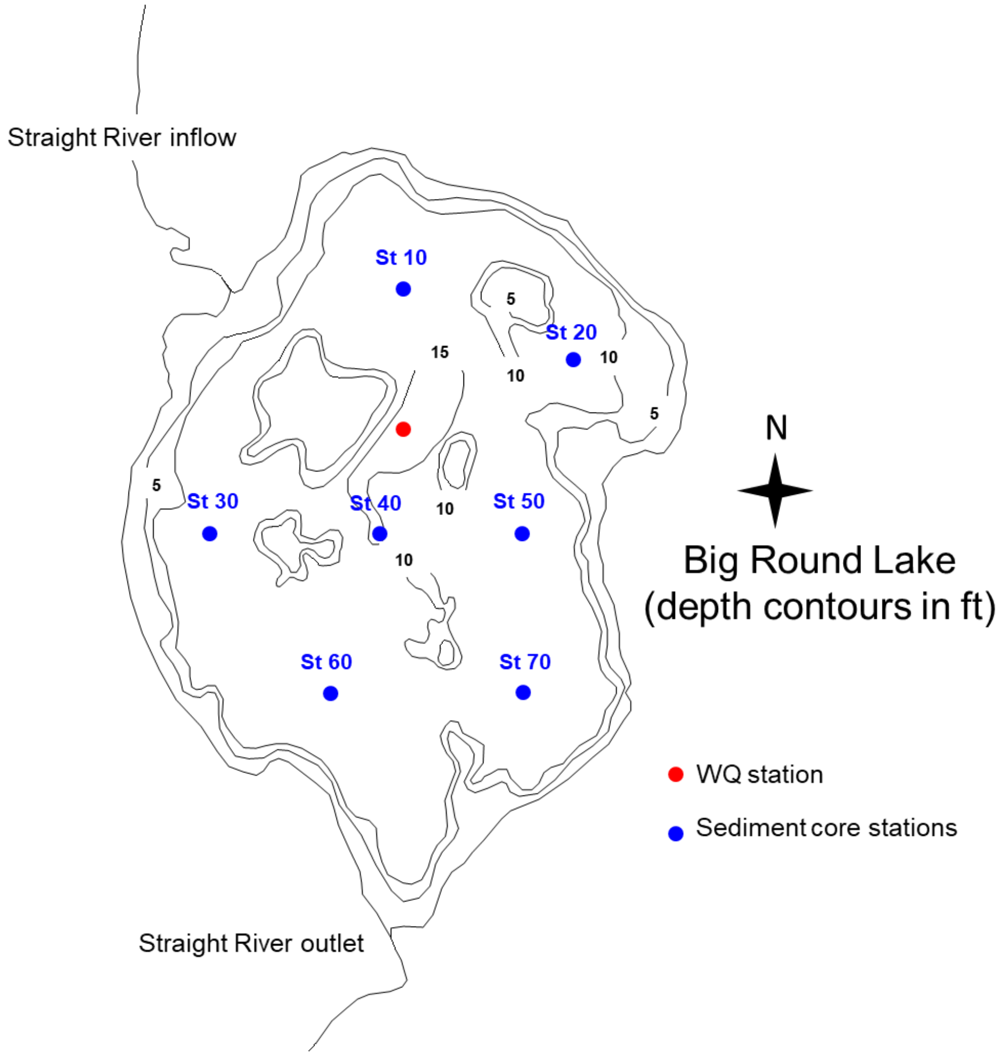

Fig. 1. Bathymetric map of Big Round Lake showing the water quality station and various sediment coring locations.

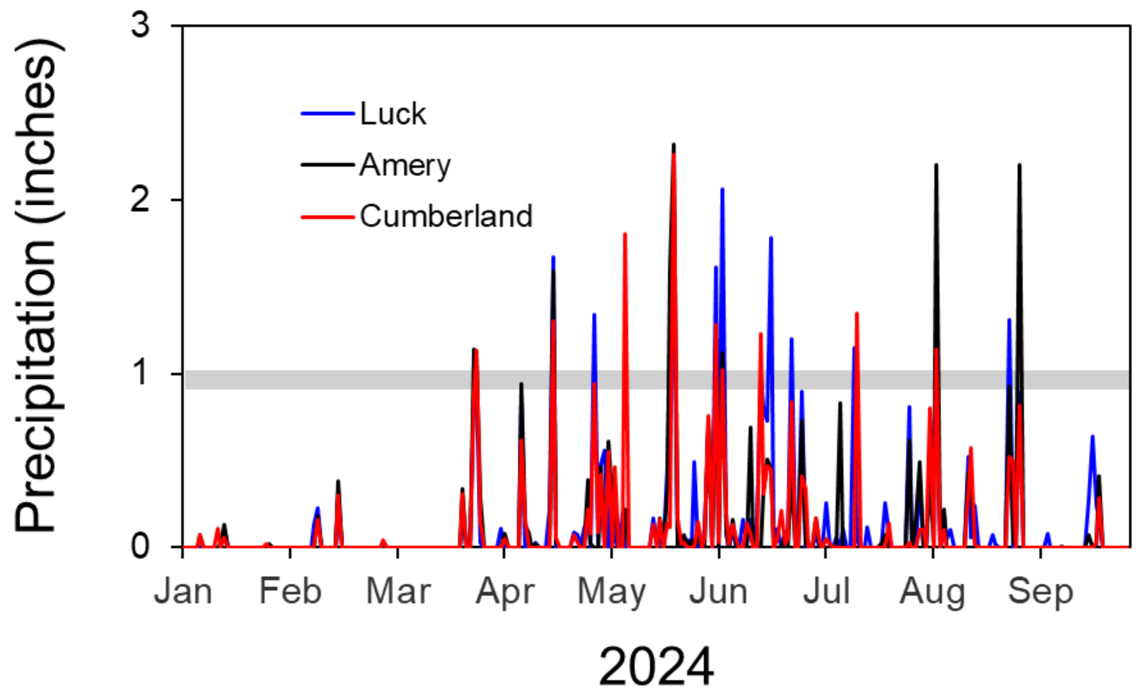

Fig. 2. Variations in seasonal precipitation measured at Luck, Amery, and Cumberland Wisconsin in 2024. Gray horizontal line denotes daily precipitation > 1 inch.

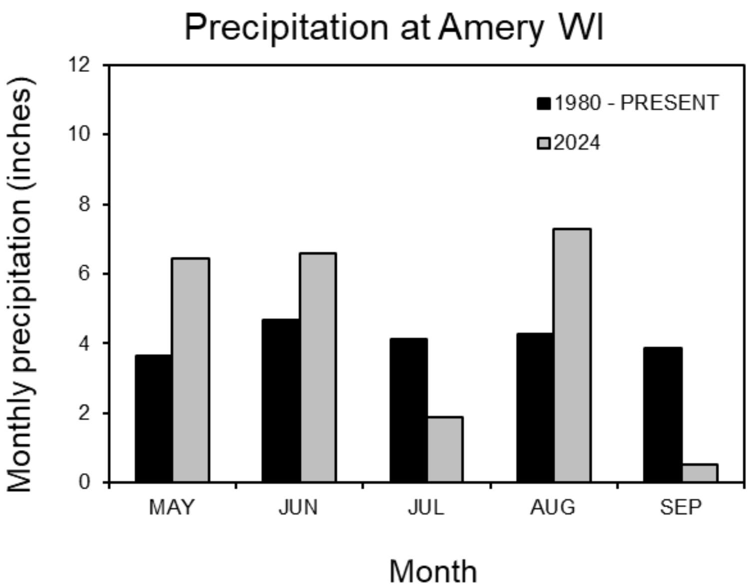

Fig. 3. Monthly variations in precipitation measured at Amery Wisconsin.

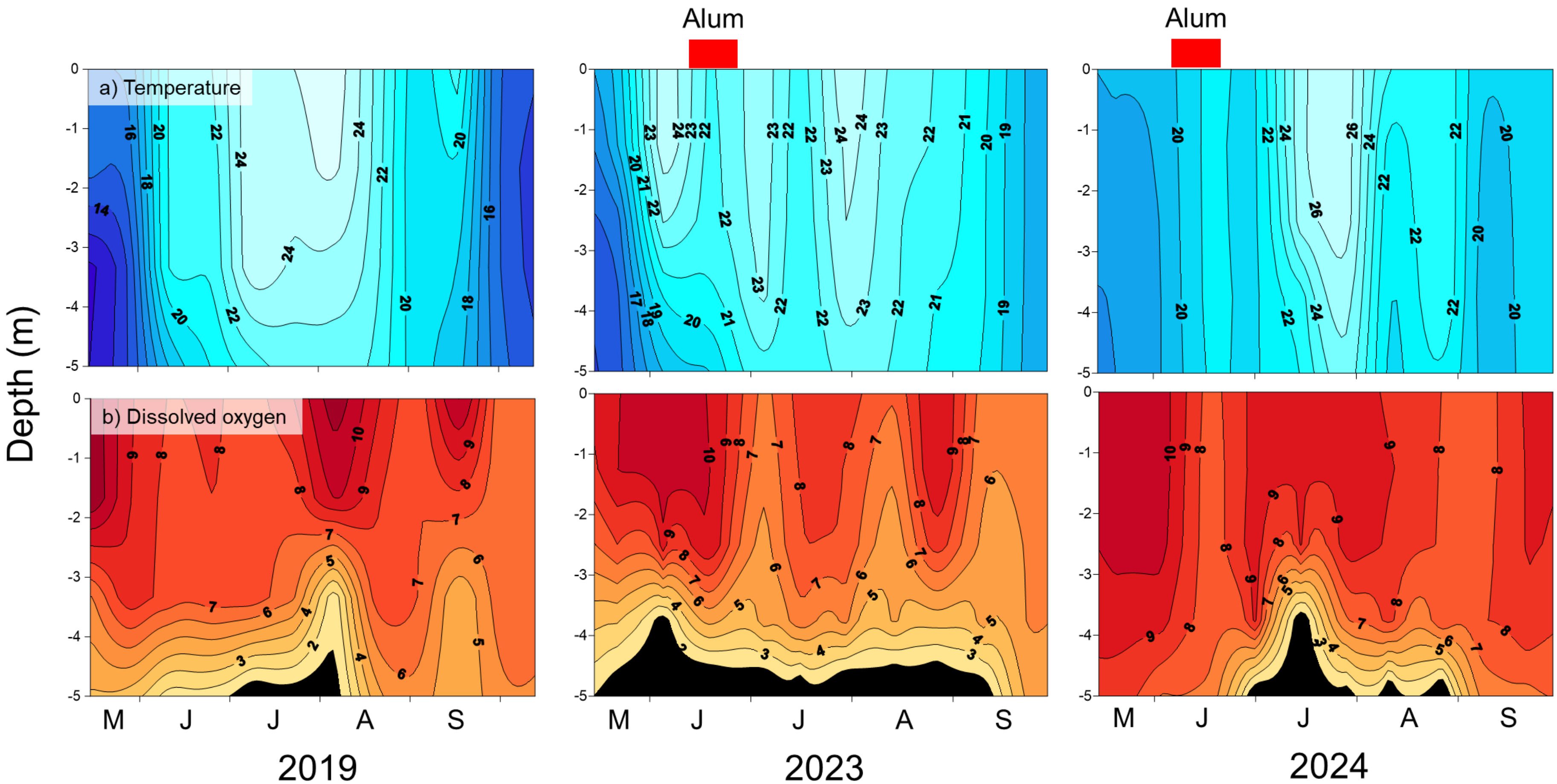

Fig. 4. Seasonal and vertical variations in water temperature (upper panels) and dissolved oxygen (lower panels) at the Big Round Lake sampling station in 2019 (pre-alum application), 2023 (1st alum application), and 2024 (2nd alum application). Black bottom area in the lower panel represents the period of hypolimnetic anoxia.

Fig. 5. Seasonal variations in bottom total and soluble phosphorus (P) in 2019 (pre-alum application, 2023 (1st alum application), and 2024 (2nd alum application). Horizontal red bar denotes the period of the alum application in 2023 and 2024.

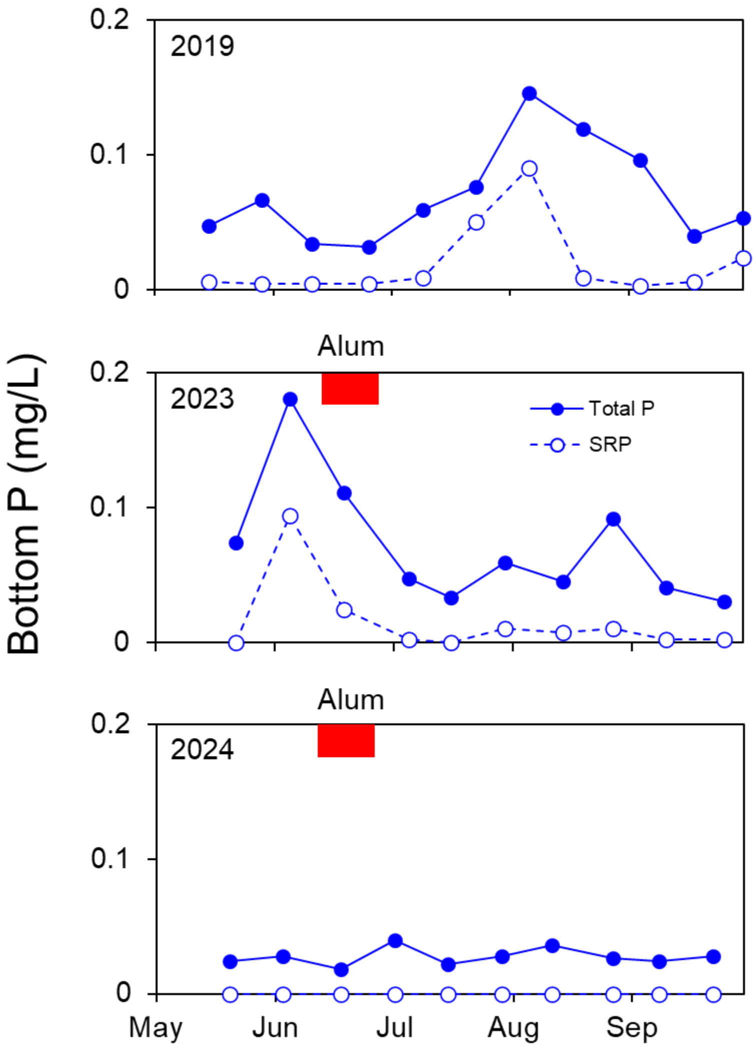

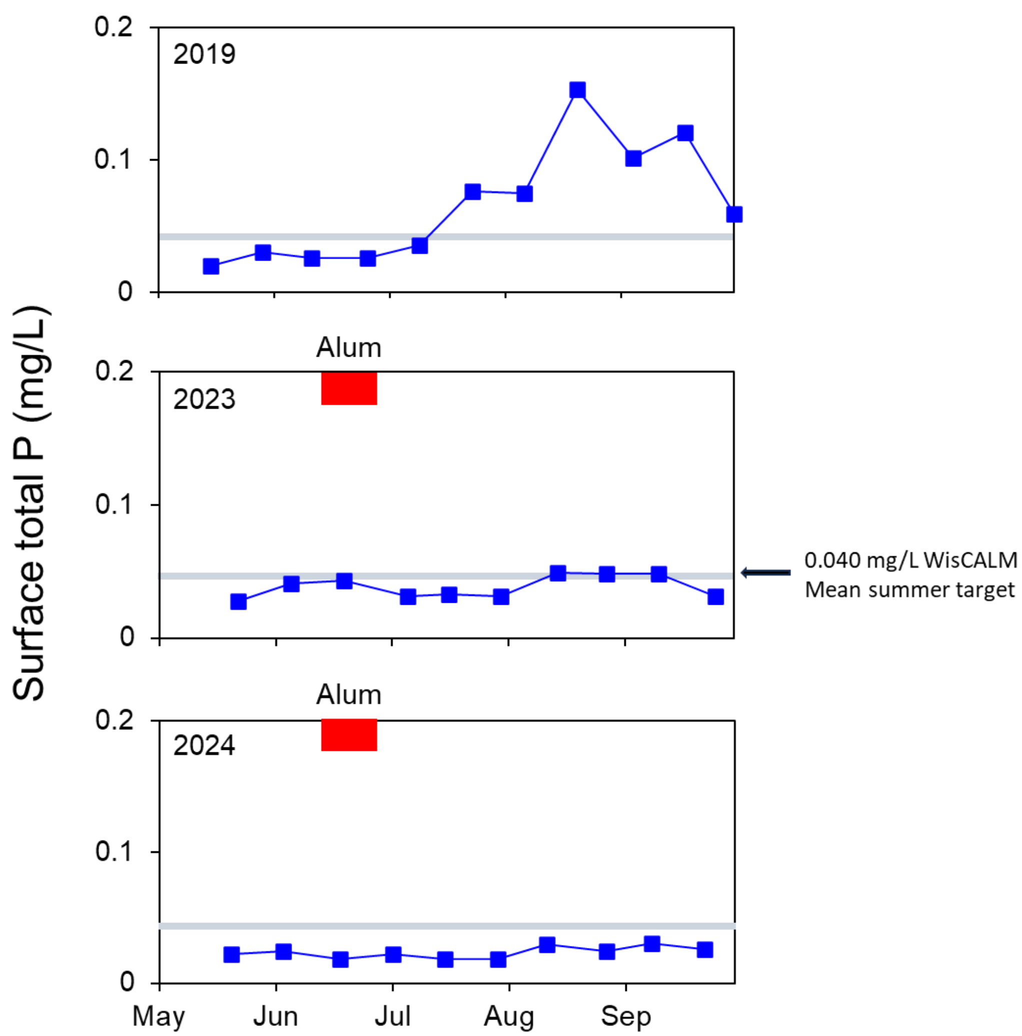

Fig. 6. Seasonal variations in surface (upper 2-m integrated depth) total phosphorus (P) in 2019 (pre-alum application), 2023 (1st alum application), and 2024 (2nd alum application). Horizontal red bar denotes the period of the alum application in 2023 and 2024.

Fig. 7. Seasonal variations in surface (upper 2-m integrated depth) chlorophyll in 2019 (pre-alum application), 2023 (1st alum application), and 2024 (2nd alum application). Horizontal red bar denotes the period of the alum application in 2023 and 2024.

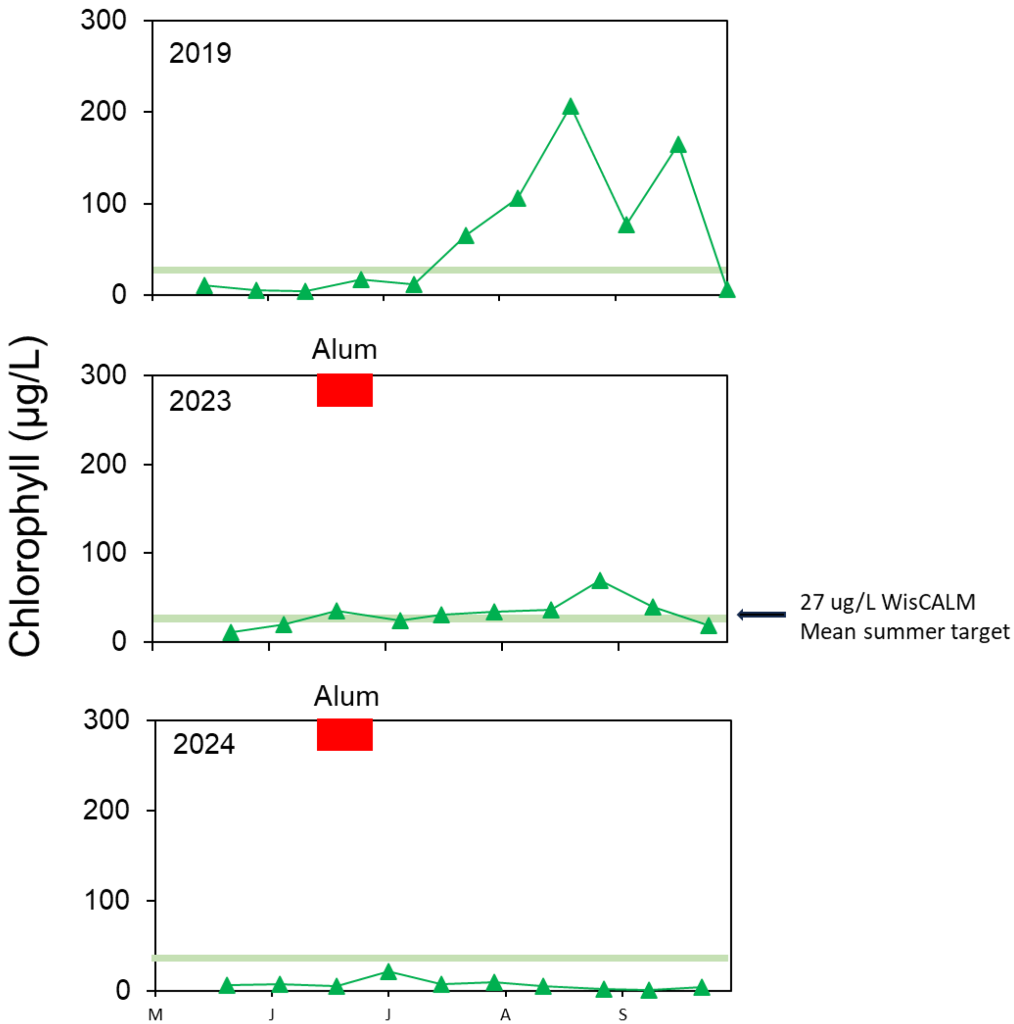

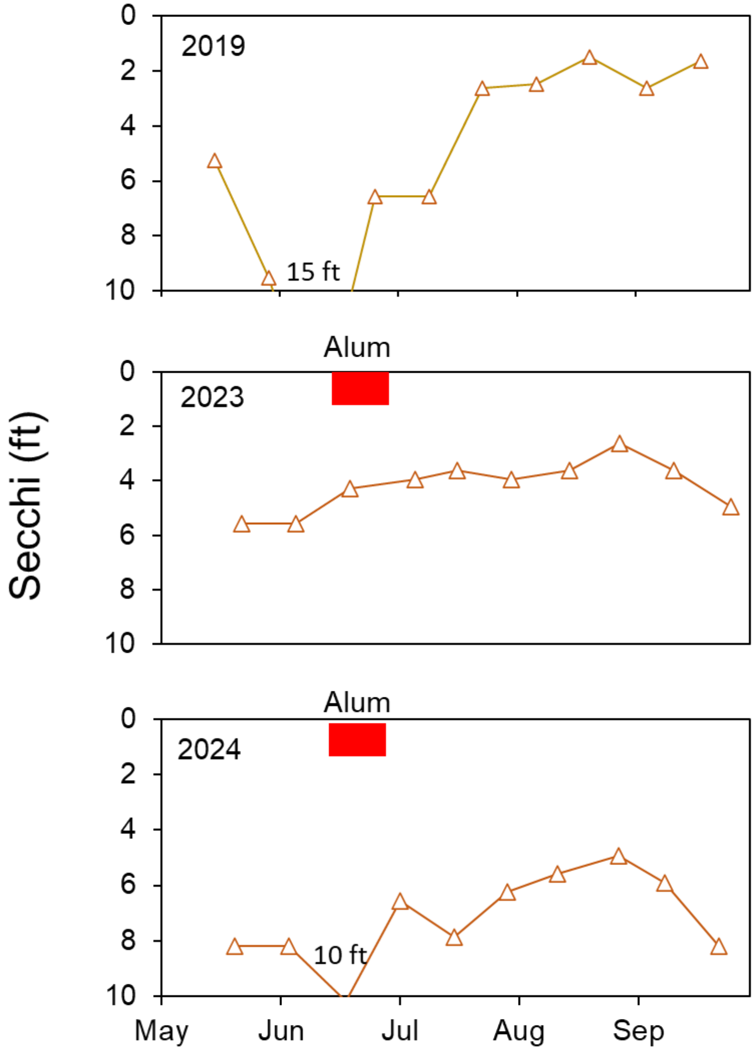

Fig. 8. Seasonal variations in Secchi transparency in 2019 (pre-alum application), 2023 (1st alum application), and 2024 (2nd alum application). Horizontal red bar denotes the period of the alum application in 2023 and 2024.

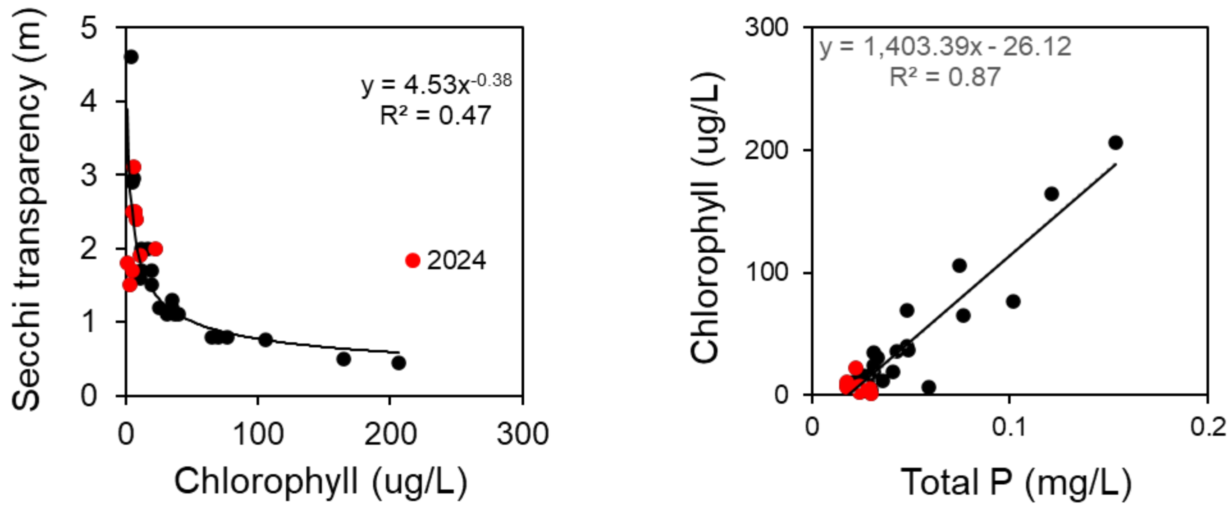

Fig. 9. Relationships between limnological trophic state variables.

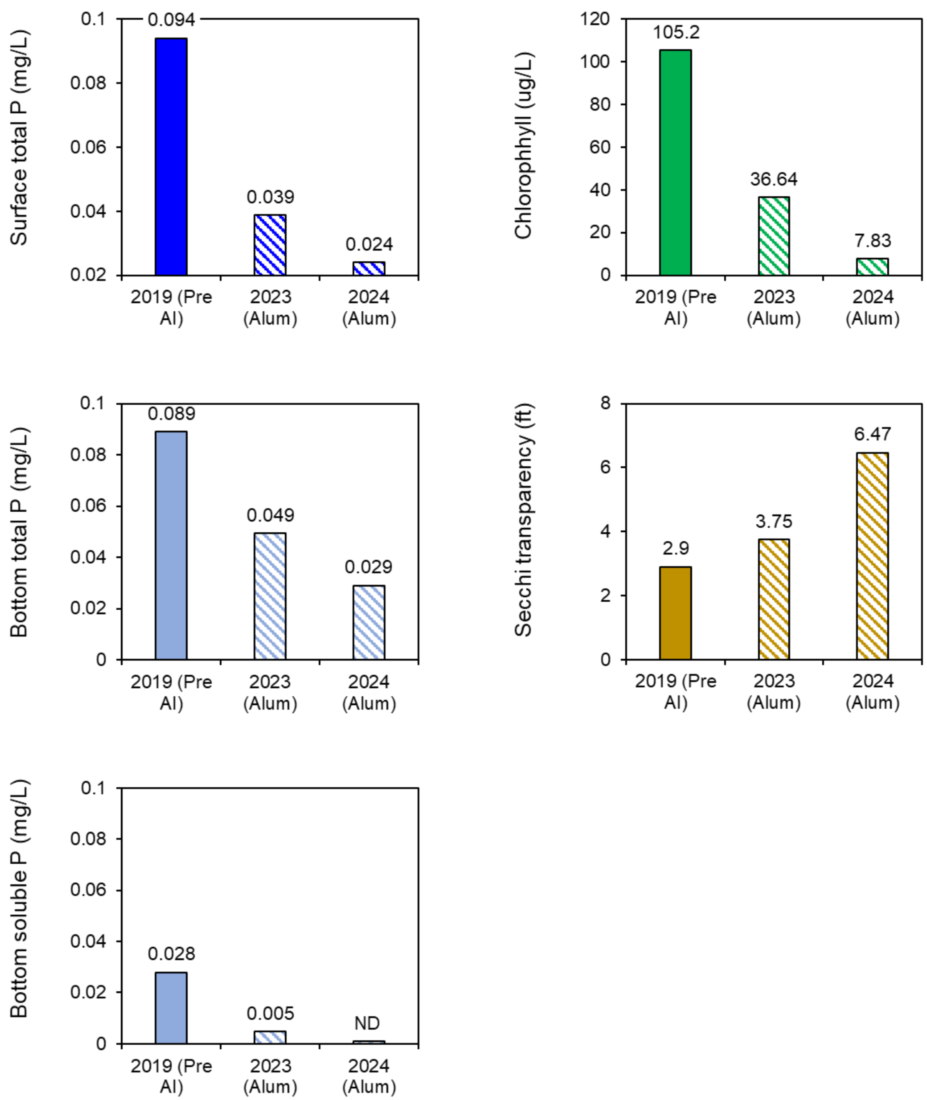

Fig. 10. Variations in mean summer (JUL-SEP) limnological response variables (surface total P, Bottom total and soluble P, chlorophyll, and Secchi transparency) in 2019 (pre-alum application), 2023 (1^{st} alum application), and 2024 (2^{nd} alum application).

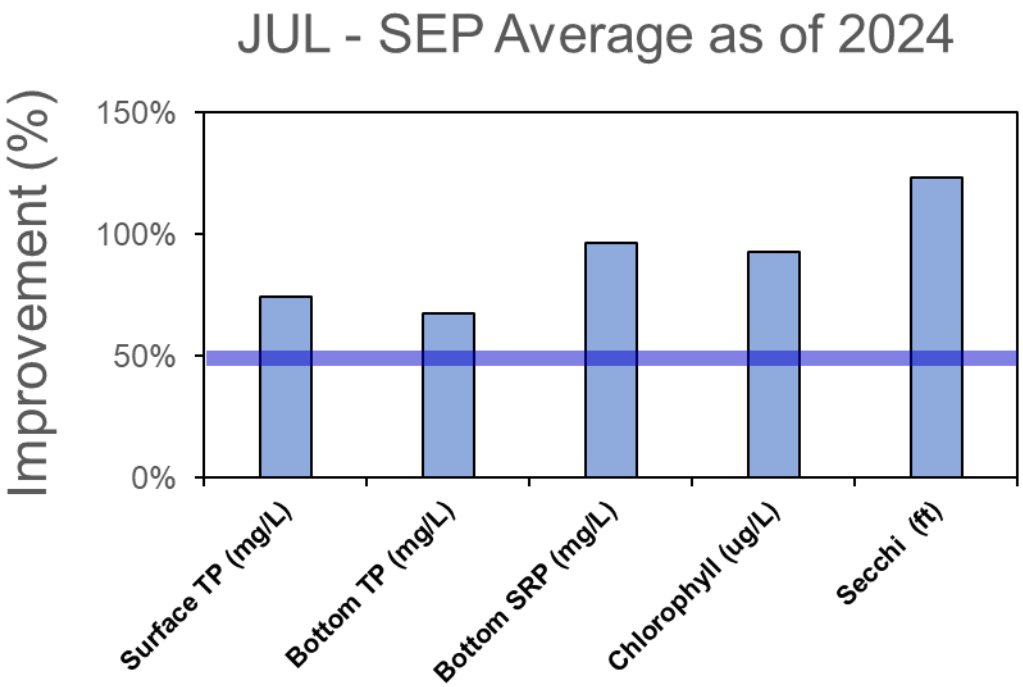

Fig. 11. Percent improvement in summer (JUL-SEP) limnological response variables in 2024 in conjunction with the second alum treatment. Percent improvement was calculated as the change or difference between 2019 versus 2024 summer means.

Fig. 12. Comparisons in monthly surface total phosphorus (upper panel), chlorophyll (middle panel), and Secchi transparency (lower panel) in 2019 (pre-alum application), 2023 (1st alum application), and 2024 (2nd alum application).

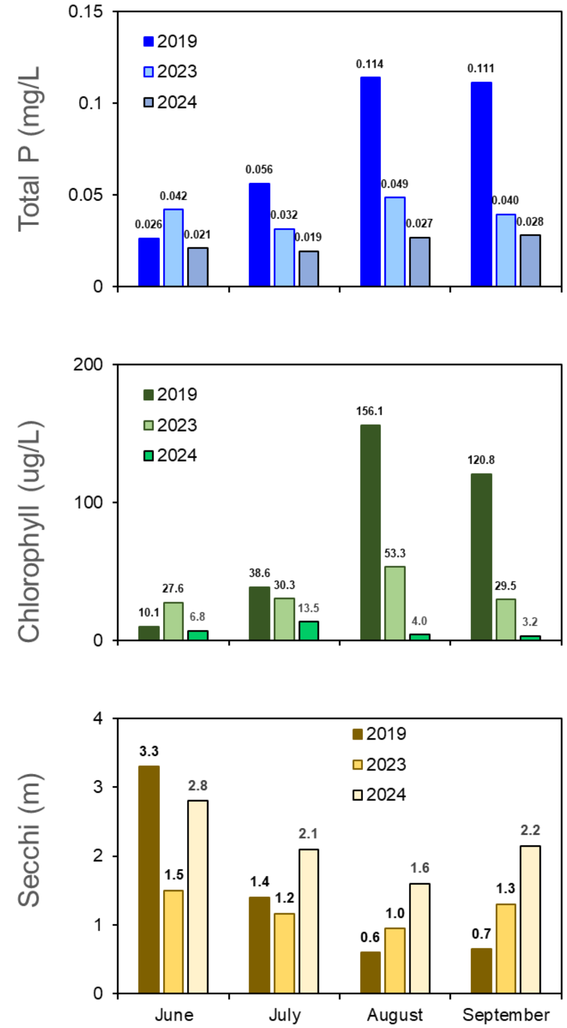

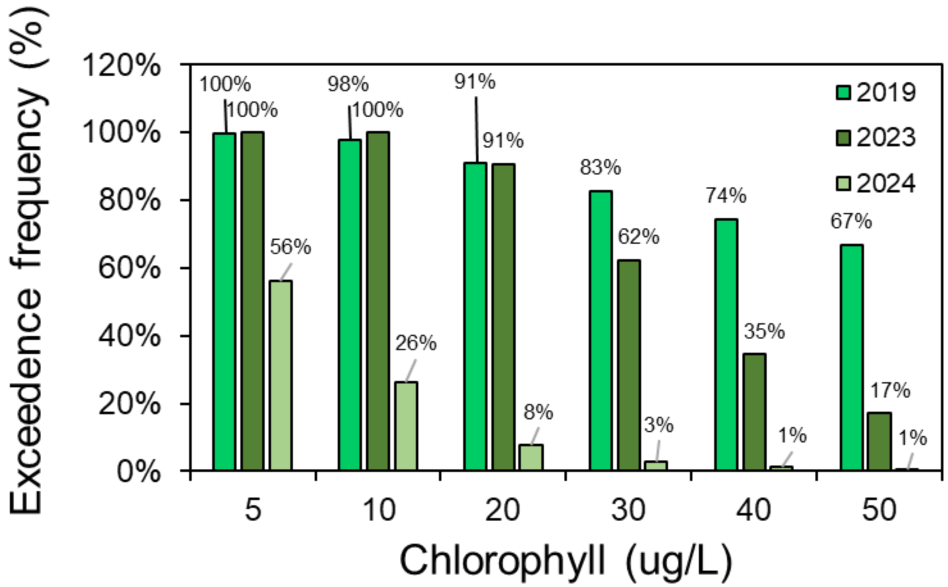

Fig. 13. Percent of the time in the summer that chlorophyll exceeded 5 µg/L, 10 µg/L, 20 µg/L, 30 µg/L, 40 µg/L, and 50 µg/L in 2019 (pre-alum treatment), 2023 (1st alum application), and 2024 (2nd alum application).

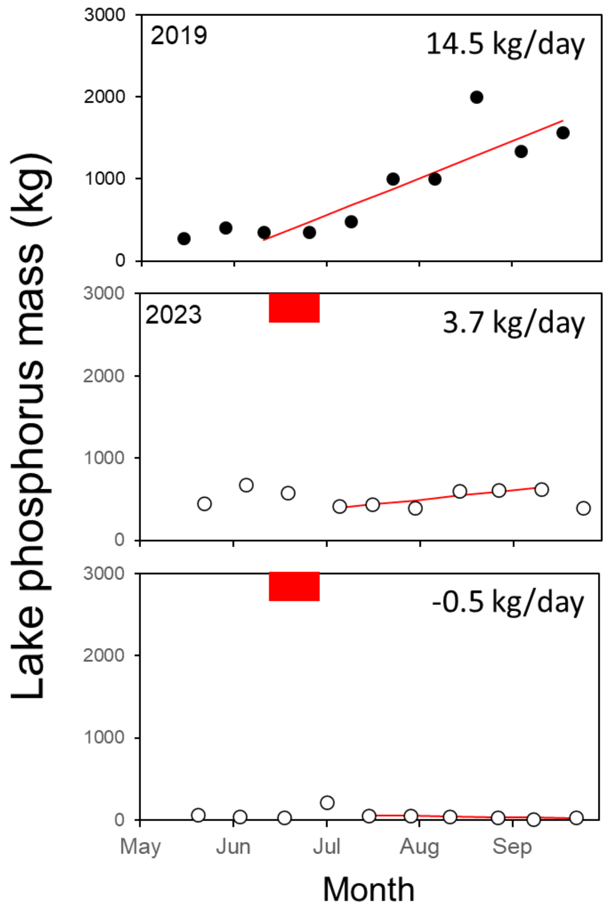

Fig. 14. Changes in lakewide total phosphorus (P) mass in 2019 (before alum treatment), 2023 (1st alum application), and 2024 (2nd alum application). Horizontal red bar denotes the period of the alum application in 2023 and 2024.

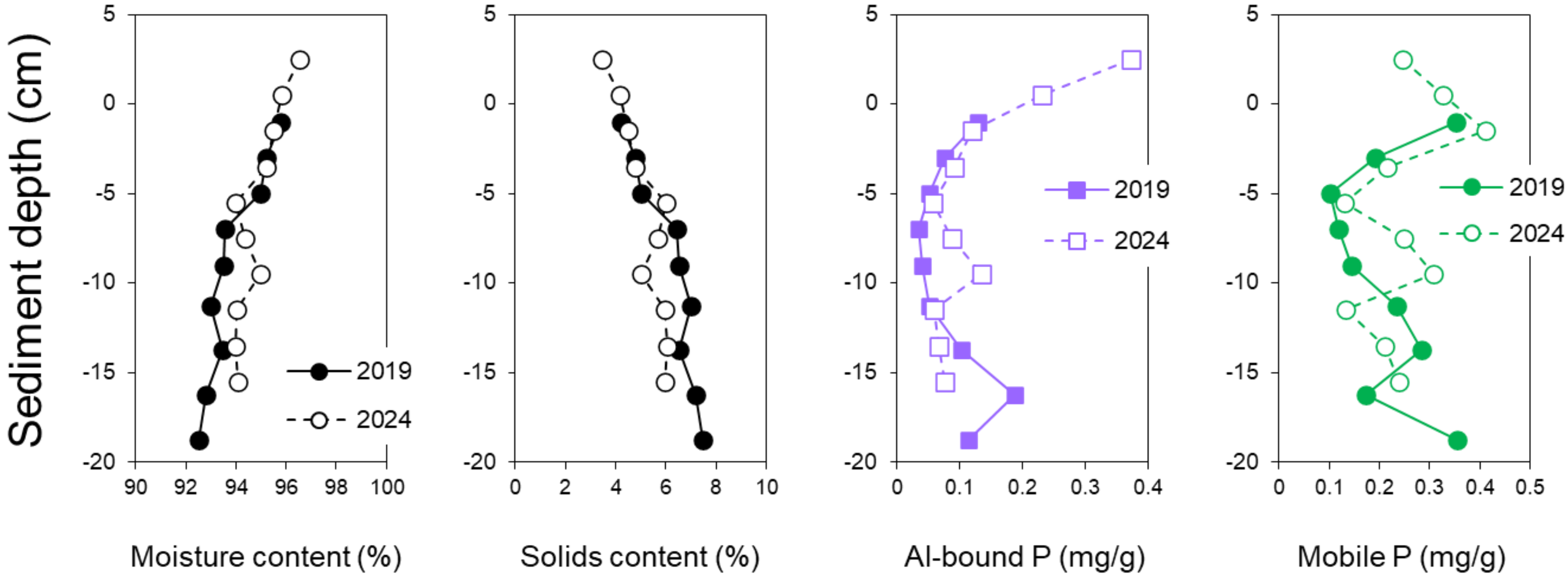

Fig. 15. Sediment vertical profiles showing changes in moisture content, solids content, aluminum-bound P, and mobile P (i.e., the sum of the loosely-bound and iron-bound P fractions) in 2019 (before alum treatment) and 2024 (after the 2nd alum application).

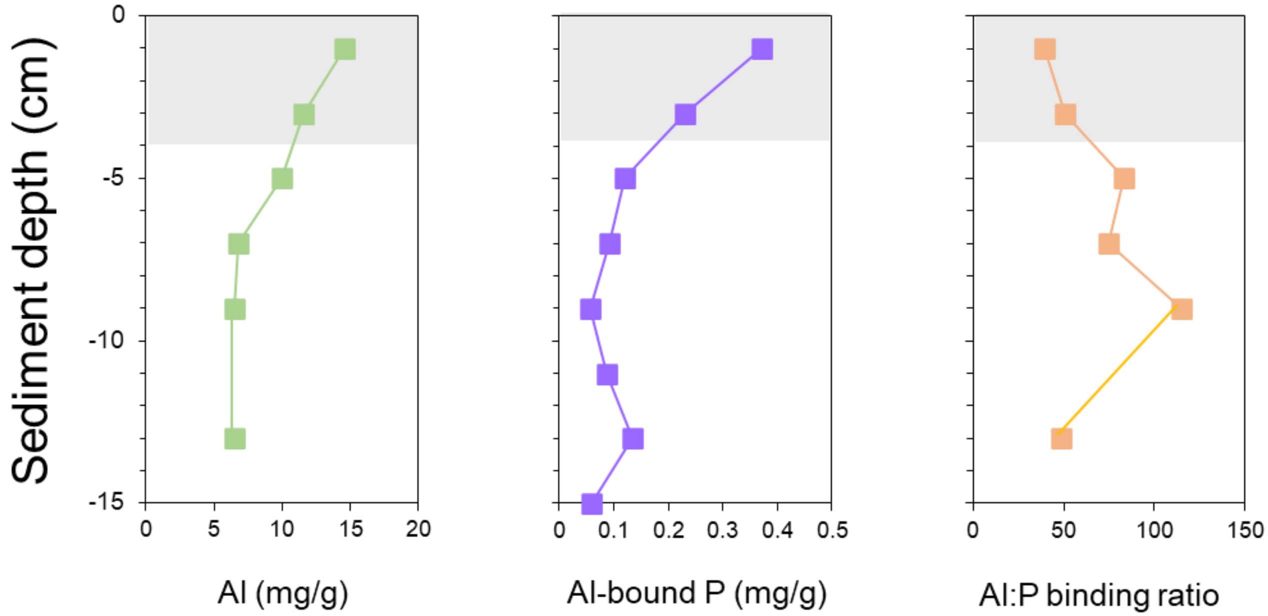

Fig. 16. Variations in sediment aluminum, aluminum-bound P, and the Al:P binding ratio for sediment collected at the WQ station in Big Round Lake in 2024. The gray area denotes the probably location of the Al floc Layer. The Al:P binding ratio represents the mass of P bound per mass of Al. An Al:P binding ratio of ~ 12:1 to 15:1 can be achieved over time as sediment P diffuses upwatrd into the Al floc.

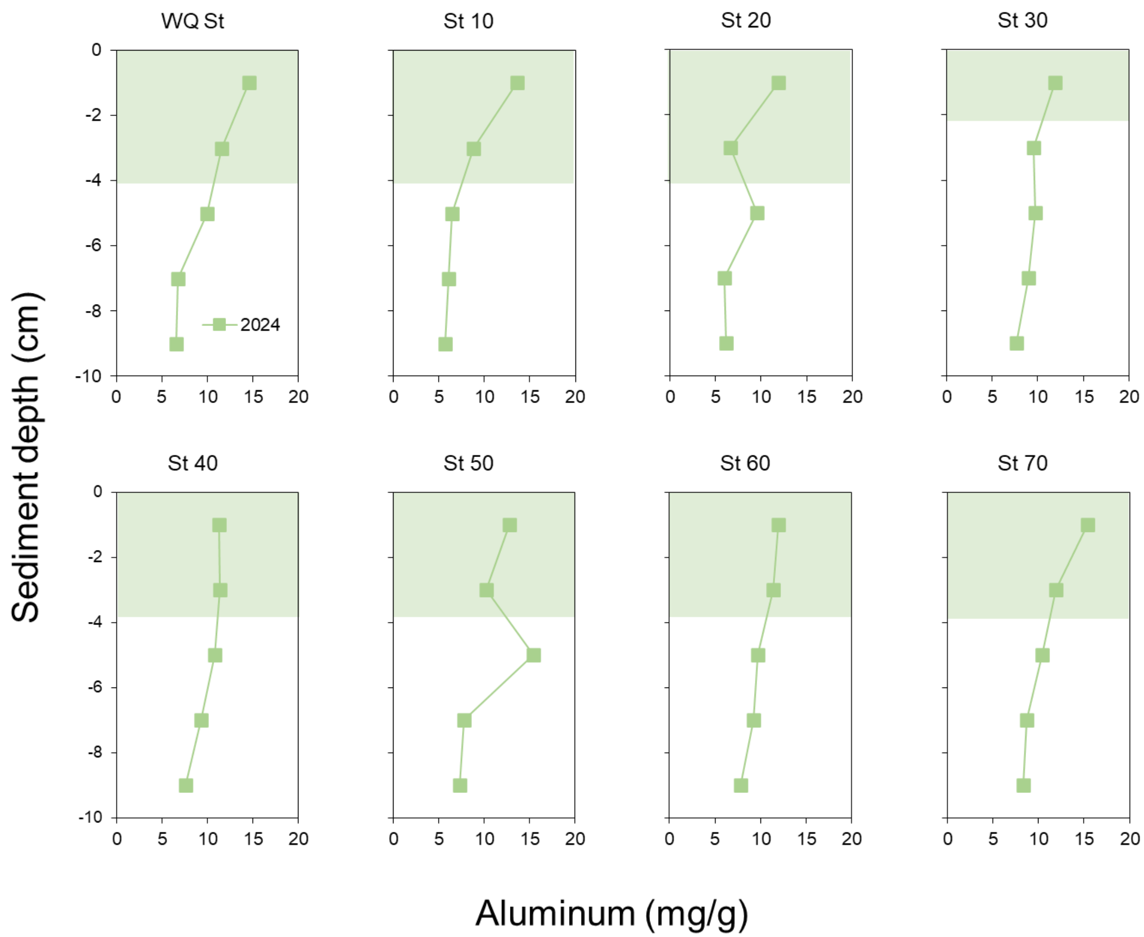

Fig. 17. Spatial variations in sediment core vertical profiles of aluminum in 2024 (i.e., after the 2nd alum application). Green shaded areas denote the location of the Al floc.

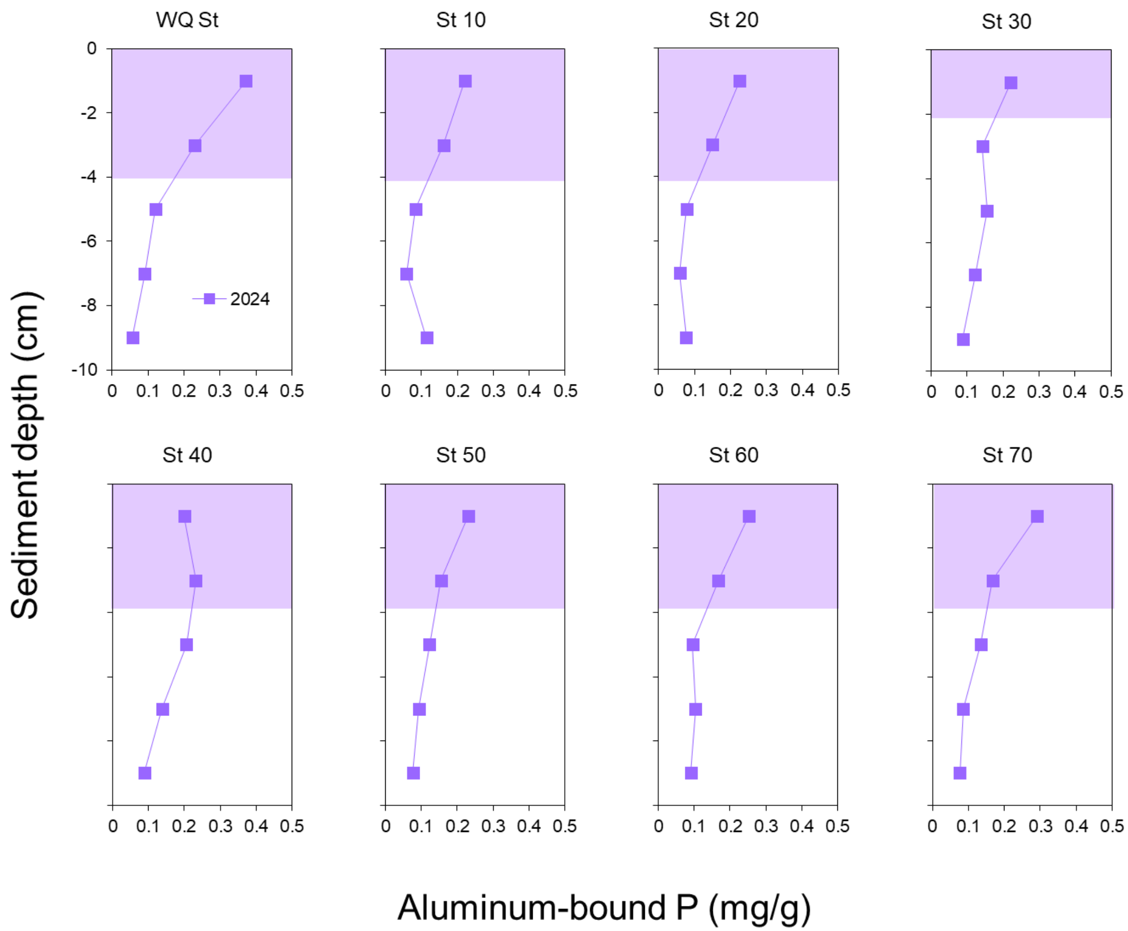

Fig. 18. Spatial variations in sediment core vertical profiles of aluminum-bound P in 2024 (i.e., after the 2nd alum application). Lavender shaded areas denote the location of the Al floc.

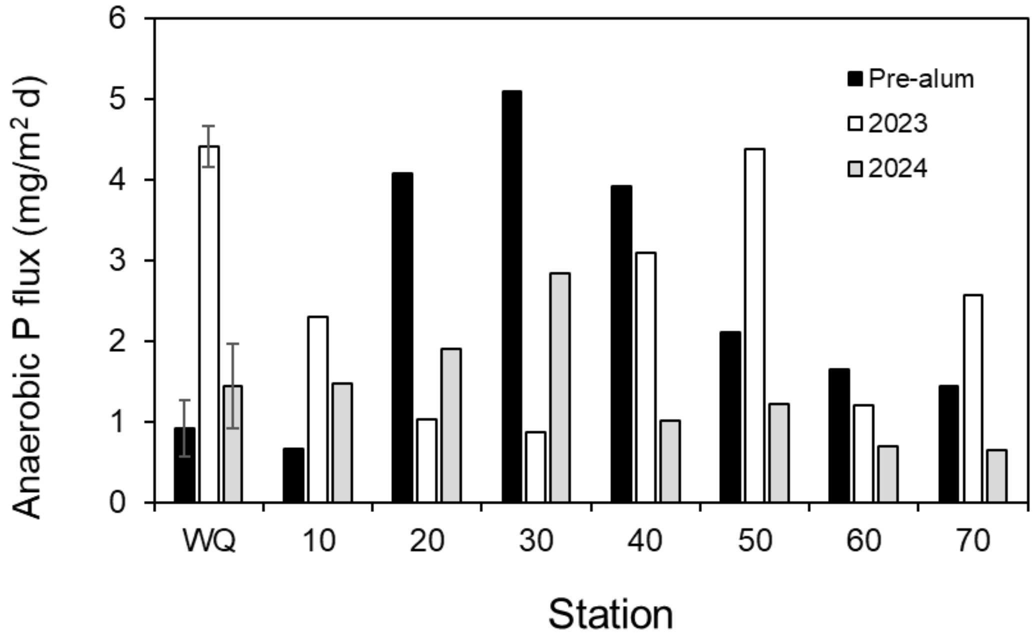

Fig.19. Laboratory-derived anaerobic diffusive P flux at various stations measured in 2019 (before alum treatment), 2023 (1st alum application), and 2024 (2nd alum application).

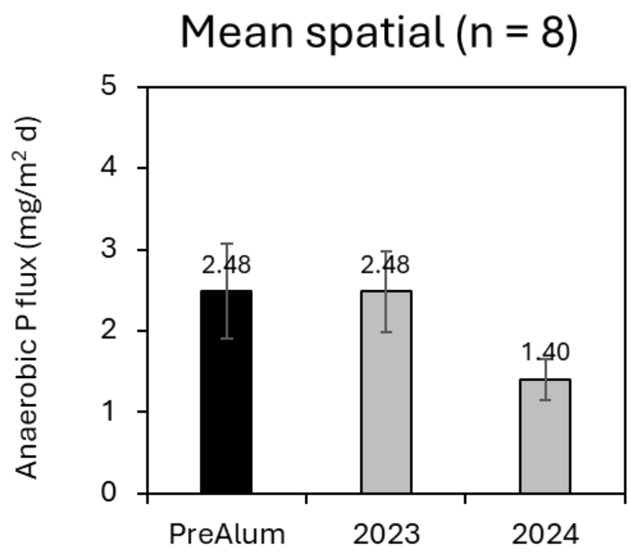

Fig.20. Mean (n = 8, ± 1 standard error) laboratory-derived anaerobic diffusive P flux in 2019 (before alum treatment), 2023 (1st alum application), and 2024 (2nd alum application).